Hydride-like $NH_2^{\delta-}$ species-driven reductive amination over Co@CoO catalyst

Wanjun Guo[1,2], Zhi-Qiang Wang[1,2], Shuang Xiang[1], Yaxuan Jing[1]*, Yong Guo[1], Xiaohui Liu[1], Xue-Qing Gong[1]* and Yanqin Wang[1]*

[1] Key Laboratory for Advanced Materials and Joint International Research Laboratory of Precision Chemistry and Molecular Engineering, Feringa Nobel Prize Scientist Joint Research Center, Research Institute of Industrial Catalysis, School of Chemistry and Molecular Engineering, East China University of Science and Technology, Shanghai, 200237, China.

[2] These authors contributed equally.

Corresponding authors: jingyaxuan@ecust.edu.cn (Y. X. J.); xgong@ecust.edu.cn (X. Q. G.); wangyaqin@ecust.edu.cn (Y. Q. W.)

Abstract

Selective synthesis of primary amines via reductive amination becomes an important research topic due to their wide applications. Various metal-based catalysts (Ru, Ir, Pt, Rh, *etc.*) have been developed; however, most systems suffer from low efficiency and poor stability. Here, we revealed that the hydride-like $NH_2^{\delta-}$ species, generated by the dissociation of NH_3 over a core-shell structured Co@CoO catalyst is capable of accelerating the ammonolysis of Schiff bases, the reaction intermediates. This catalyst can handle various reductive aminations of aldehydes and ketones under mild conditions and run 21 times without deactivation. The combination of various spectroscopic measurements and computational modelling illustrated that this catalyst not only drives the dissociation of H_2 to active $H^{\delta-}$ species, it also enables the

homolytic and heterolytic cleavages of NH_3 to $NH_2^{\delta-}$ species. D_2 isotopic tracing experiment provided further evidence of the direct participation of hydride-like $NH_2^{\delta-}$ species in the ammonolysis of the Schiff bases. Theoretical calculations also verified the stable co-adsorption state of the $H^{\delta-}$ and $NH_2^{\delta-}$ species which allows the Schiff base to move freely on the surface of the CoO shell, resulting in the exceptional catalytic activity. This study demonstrates, for the first time, the potential of metal-oxide catalysts for the production of primary amines through reductive amination.

Introduction

Amines, in particular primary amines, are widely used for the synthesis of dyes, surfactants, polymers, pharmaceuticals, and agrochemicals, profoundly shaping the landscape of the chemical industry.[1-7] In the last decades, catalytic reductive amination of biomass-derived carbonyl compounds (furfural, cyclopentanone, HMF, etc.) to obtain primary amines has drawn particular attention, providing grand opportunities for the sustainable production of amines from renewable energy[1,2,5,8-13]

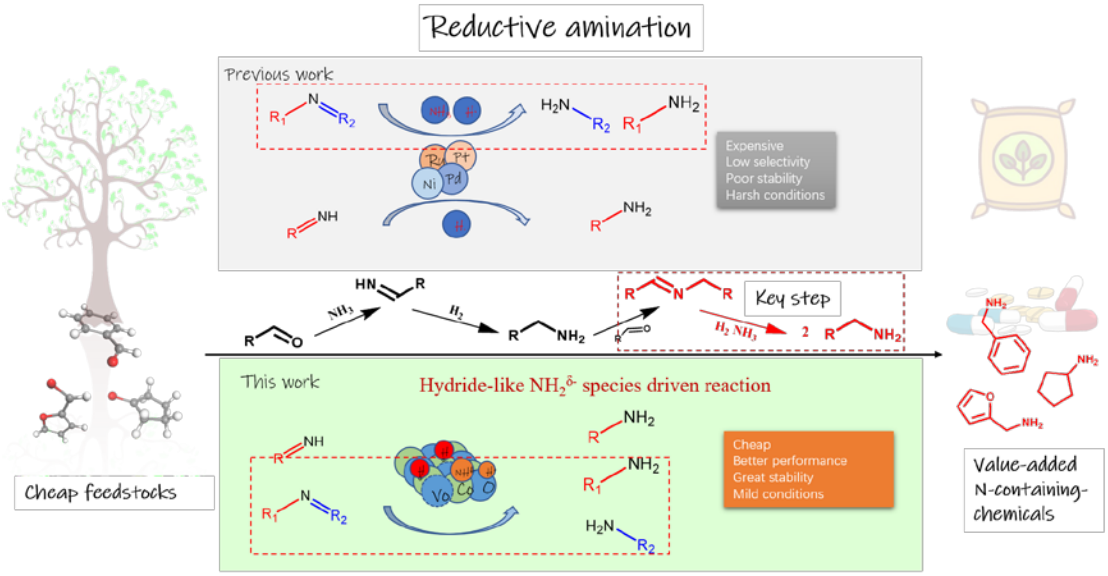

Scheme 1. Comparison of catalytic mechanisms between noble metal catalysts and Co@CoO.

The reductive amination of carbonyl compounds undergoes the direct amination of aldehydes/ketones with NH_3 to imines and its subsequent hydrogenation. In the process, the formation of Schiff bases is inevitable through the dehydration of substrate and primary amines due to the stronger nucleophilicity of primary amine products than that of NH_3.[14-17] Previous studies demonstrated that Schiff bases were accumulated in large quantities at the beginning and then converted into corresponding primary amines, directly determining the rate of the reductive amination.[14,17] Noteworthy, the Schiff bases intermediates require the further ammonolysis to boost the selective production of primary amine products. Therefore, a key challenge of this task is to design a catalyst that enables the dissociation of NH_3. Meanwhile, with the help of H species dissociated on the designed catalyst, the highly efficient and selective production of primary amine products can be achieved.

Reductive amination was usually catalyzed by supported metal (Ru, Ir, Pt, Rh, Ni, *etc.*) catalysts.[17-29] It is widely recognized that the free radicals (H·) generated by homolytic dissociation of H_2 on the metallic species of these catalysts participate in the hydrogenation of imine during reductive amination.[30] Compared with the H· species, the $H^{\delta-}$ species generated through heterolytic dissociation of H_2 on single atom catalysts or metal oxide catalysts with oxygen vacancies were recently proved to have better catalytic performance.[31-35] Inspired by the catalysis involving $H^{\delta-}$ species, exploration on hydride-like $NH_2^{\delta-}$ species generated over metal oxide catalysts to facilitate reductive amination is of strong interest. Very recently, we found that a core-shell structured Co@CoO catalyst with CoO shell having oxygen vacancy is the real active site and enables the dissociation of H_2 to yield active $H^{\delta-}$ species.[36] Along this line, the potential of the CoO shell to drive the dissociation of NH_3 deserves special attention.

Here, we found that the hydride-like $NH_2^{\delta-}$ species dissociated on a core-shell structured Co@CoO catalyst favors the reductive amination. This catalyst is efficient for the reductive amination of various substrates to produce corresponding primary amines, outperforming most of the metal-based catalysts. Through density functional theory (DFT) calculations and D_2 isotopic experiments, we provided the direct evidence that hydride-like $NH_2^{\delta-}$ species was indeed involved in ammonolysis of the Schiff bases and an in-depth understanding of why the hydride-like $NH_2^{\delta-}$ species can promote the reductive amination so efficiently from molecule collision theory.

Results and discussion

Identification of core-shell structure of Co@CoO

The core-shell structured Co@CoO catalyst was prepared with co-precipitation followed by reduction at 250 °C for 2h under 10%H_2-90%Ar atmosphere. The characterizations by XRD, TEM and EPR were collected in Figure 1 to confirm its structure and surface property. The broad peaks at 41.6 ° and 47.5° are assigned to (100) and (101) planes of Hexagonal Cobalt (JCPDS 05-0727), and the peaks at 44.2° and 75.8° are attributed to (111) and (220) planes of Cubic Cobalt (JCPDS 15-0806). Two weak diffraction peaks at 36.5° and 61.5° are corresponded to (111) and (220) of cubic CoO (JCPDS 43-1004). These observations suggest that Co and CoO co-exist in the catalyst (Figure 1a). The TEM image shows that the outer surface exposes the crystal plane of CoO and the inside presents the structure of Cubic and Hexagonal Co, clearly proving its core-shell structure (Figure 1b). Furthermore, X-band continuous wave electron paramagnetic resonance (EPR) spectrum was collected at 77 K to detect the oxygen vacancy of Co@CoO (Figure 1c). The signal at g=2.00 is assigned to the

oxygen vacancies, demonstrating its rich surface oxygen vacancies. In short, the above all results confirmed that Co@CoO presents a core-shell structure and the CoO shell is decorated with oxygen vacancies.

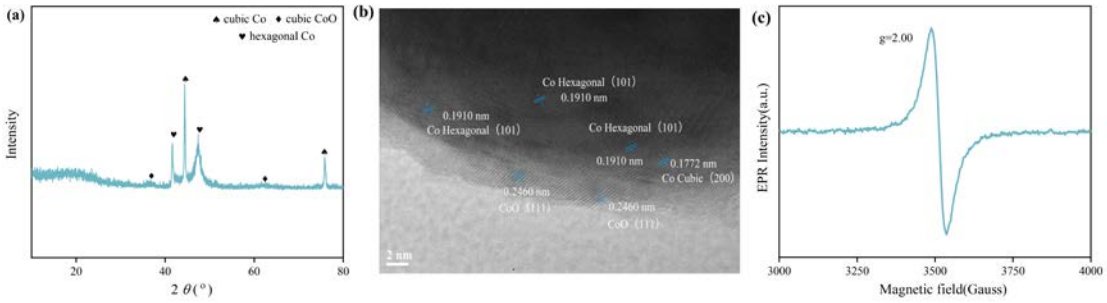

Fig. 1. Characterizations of Co@CoO. (a) XRD pattern; (b) TEM image and (c) X-band EPR spectrum recorded at 77 K.

Identification of dissociation of H_2 and NH_3 over Co@CoO

Then, in-situ DRIFTS experiments were conducted to verify the dissociation of H_2 and explore the dissociation of NH_3 on the Co@CoO surface (Figure 2a and 2b). Upon the introduction of H_2 into the gas cell, the band at 1000 cm^{-1} assigning to the Co-H band appeared, indicating the dissociation of H_2 on the CoO shell (Figure 2a). When introducing D_2 gas into the gas cell, the Co-H band and the O-H stretching vibration peaks disappeared, meanwhile the peak of O-D bonding at 2000-2600 cm^{-1} appeared, accordingly confirming that the heterolytic cleavage of H_2 really occurs on the CoO surface of Co@CoO catalyst, in good agreement with our previous finding. [36]

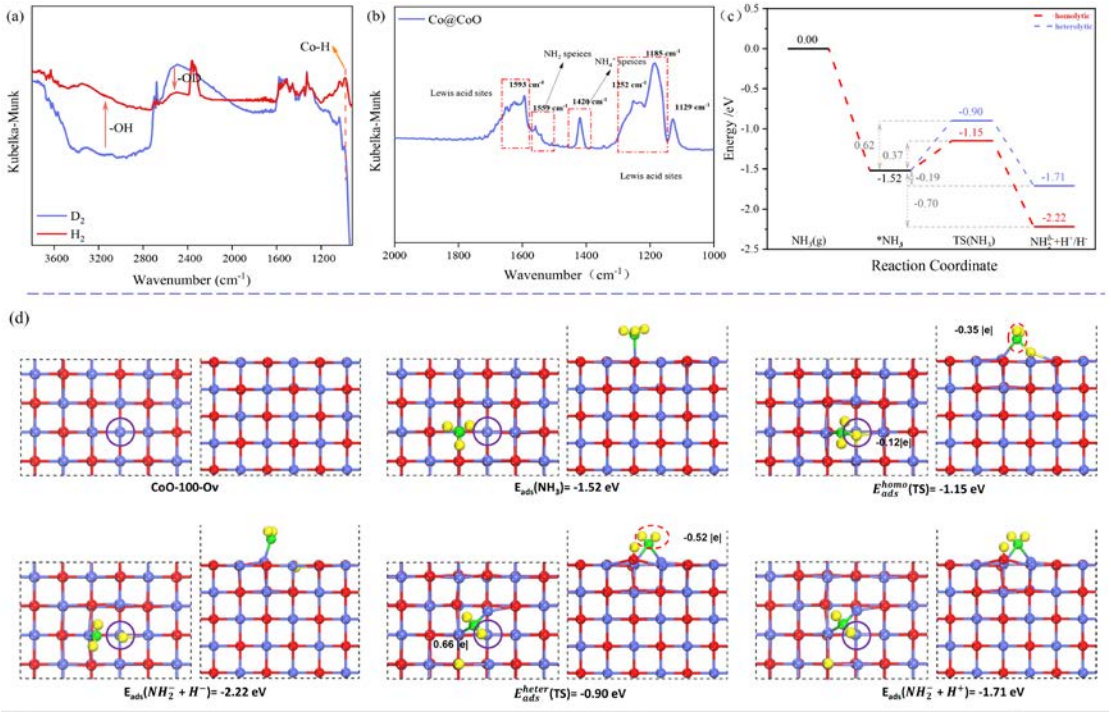

Fig. 2. (a) In situ DRIFTS of Co@CoO under H_2/D_2 gas atmosphere. (b) NH_3-adsorption DRIFT spectra of Co@CoO. (c-d) Calculated structures of homolysis and heterolytic NH_3 on CoO (100)； Adsorption NH_3, TS of homolysis NH_3 (E_{ads}^{homo}(TS)), TS of heterolytic NH_3 (E_{ads}^{heter}(TS)), final state of homolysis NH_3 (NH_2^- +H$^-$), and final state of heterolytic NH_3 (NH_2^- +H$^+$).

With the introduction of NH_3 gas into the gas cell (Figure 2b), six bands were clearly distinguished: the bands at 1593 cm^{-1}, 1252 cm^{-1} and 1185 cm^{-1} are assigned to the molecule NH_3 coordinated to an electron-deficient metal atom (CoOx species)[37]; the peak at 1129 cm^{-1} is ascribed to the hydrogen bonding formed by the coupling of nitrogen atom with hydrogen of surface hydroxyl groups; and the band at 1420 cm^{-1} is considered to be NH_4^+ ions produced by the coupling of surface Brönsted sites with NH_3.[38,39] Importantly, the band at 1559 cm^{-1} corresponding to the $NH_2^{\delta-}$ species appeared, clearly signifying that NH_3 is dissociated to afford the surface Co-NH_2 and O-H species over the CoO shell.[38,40-42] These findings provide strong evidence that the CoO shell indeed enables the dissociation of H_2 and NH_3 simultaneously. We

suspected that the dissociated hydride-like $NH_2^{\delta-}$ species are favorable for the Schiff base ammonolysis, thus resulting in the superior activity of Co@CoO catalyst.

Next, DFT calculations (Figure 2c and Figure 2d) were performed to comparatively investigate the homolytic and heterolytic cleavage of NH_3 over CoO (100) with oxygen vacancies. For the homolytic cleavage of NH_3 to $H^{\delta-}$ and hydride-like $NH_2^{\delta-}$, the process is strongly exothermic by 0.70 eV and gives a barrier of only 0.37 eV, indicating its great feasibility in both thermodynamics and kinetics. By sharp contrast, the heterolytic cleavage to $H^{\delta+}$ and hydride-like $NH_2^{\delta-}$ is only exothermic by 0.19 eV and has to overcome a higher barrier of 0.62 eV. Comparison of the two energy profiles clearly demonstrates that over the CoO shell, the homolytic cleavage of NH_3 to $H^{\delta-}$ and hydride-like $NH_2^{\delta-}$ is of obvious dominance compared with the heterolytic cleavage.

Activity and stability of Co@CoO in reductive amination

The above results confirm that the core-shell structured Co@CoO catalyst with oxygen vacancies enables the homolytic cleavage of NH_3 to $H^{\delta-}$ and hydride-like $NH_2^{\delta-}$. The catalytic performance of this unique Co@CoO catalyst for the reductive amination was tested and three common reductive aminations of biomass-derived compounds (cyclopentanone, benzaldehyde and furfural) over Co@CoO were investigated (Figure 3a). For the reductive aminations of cyclopentanone and benzaldehyde, Co@CoO shows two times higher productivities and lower temperatures than that of any other reported metal-based catalysts, including noble-metal-based catalysts. For the reductive amination of furfural, Co@CoO also outperforms most of the metal-based catalysts and its productivities is only lower than that of $Ru_1/NC/Nb_2O_5$, a single-atom catalyst since $Ru_1/NC/Nb_2O_5$ allows the maximum possible atom economy. Although Raney

Co shows a slight advantage in productivities, higher temperature is required to overcome the reaction energy barrier. Unequivocally, these results clearly demonstrate the overwhelming efficiency of Co@CoO catalyst compared with almost all emerging metal-based catalysts in common reductive aminations, probably because of its unique role of hydride-like $NH_2^{\delta-}$ species dissociated on the CoO shell. Applicability of Co@CoO towards the reductive amination of various substituents including aromatic and aliphatic aldehydes/ketones was also investigated (Figure 3b). Encouragingly, Co@CoO affords high yields (>94%) of primary amines for all reactions tested. Noteworthy, the conversion of aromatic aldehydes/ketones with electron-withdrawing and minor electron-donating substituents, such as F, Cl, Br and CH_3O species, worked well in high yields of 94%-96%. Moreover, desired reactivity was achieved when the aliphatic aldehydes and ketones with various aliphatic chains as the substrates. Even Co@CoO is able to perform the reductive amination of biomass-derived furfural to furfuryl amine (98% yield), which is a significantly important process in biomass valorization, in a yield of 98%. Then we explored its application in the reductive amination of biologically active molecules, and the selective conversion of 4-, 2-methoxyphenylacetone, nabumetone and Stanolone to their corresponding primary amines was realized. In short, these results fully confirm the broad utility of Co@CoO to catalyze reductive amination.

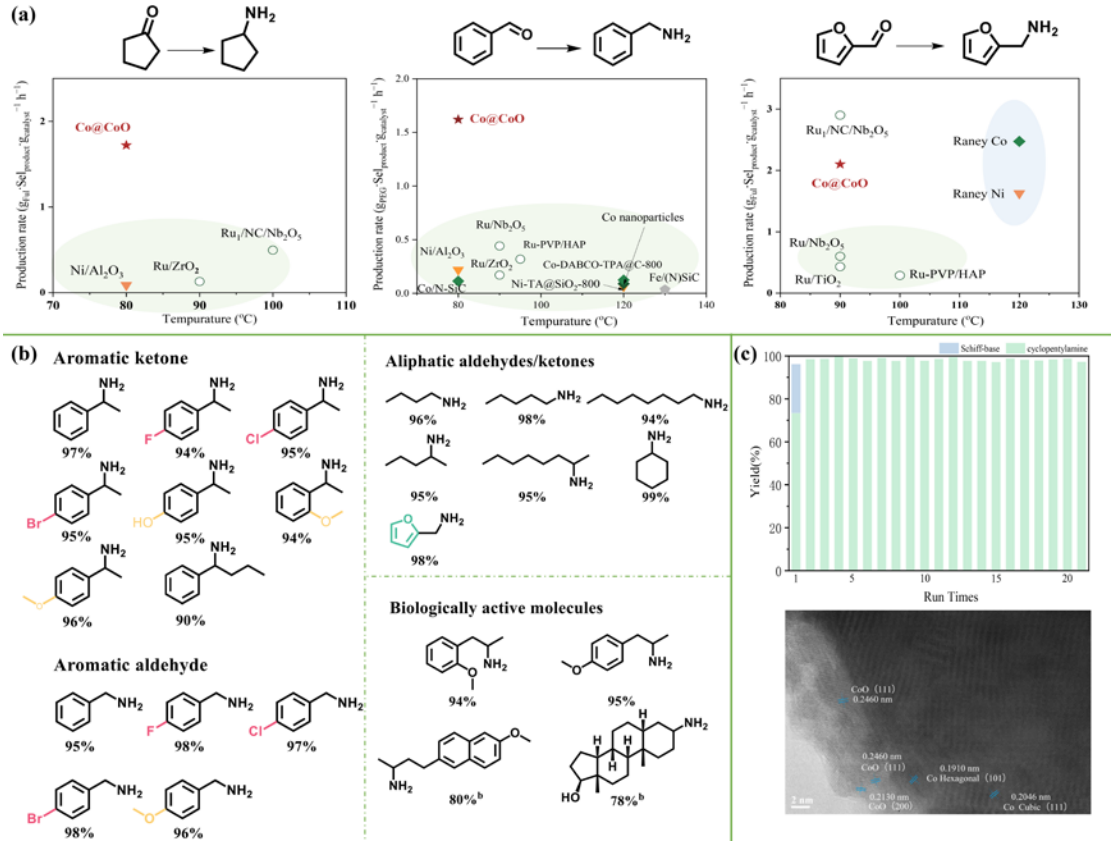

Fig. 3. (a) The catalytic performance of reductive amination between Co@CoO and other catalysts.[11,16,17,19,20,22-27,43-45] (b) Reductive amination of aliphatic substituted ketones and aldehydes to primary amines. Reaction conditions: 20 mg Co@CoO catalyst, 2 mmol substrates, 100 °C, 0.4 MPa NH_3, 2 MPa H_2, 5 ml CH_3OH, GC yield with 1,4-dioxane as internal standard; a, GC yield with 1,4-dioxane as solvent and dodecane as internal standard; b, isolated yields of converted hydrochloride salts. (c) Catalyst stability of Co@CoO for the amination of cyclopentanone and the TEM image of the 21 times-used catalyst.

Considering the simple structure of cyclopentanone, its conversion was selected as a probe reaction to study the catalyst stability and catalytic mechanism. We performed the stability test of Co@CoO and found that the catalyst can be reused 21 times without any deactivation in catalytic performance (Figure 3c). Interestingly, the activity has increased after the first test, probably because the catalyst undergoes surface reconstruction to generate more active surface sites. TEM images (Figure 3c and Figure 1b) show no obvious difference

between fresh and used Co@CoO and only the CoO shell became deeper. Consequently, the great stability of Co@CoO will bring an attractive future in industrial application.

The unique role of the hydride-like $NH_2^{\delta-}$ species

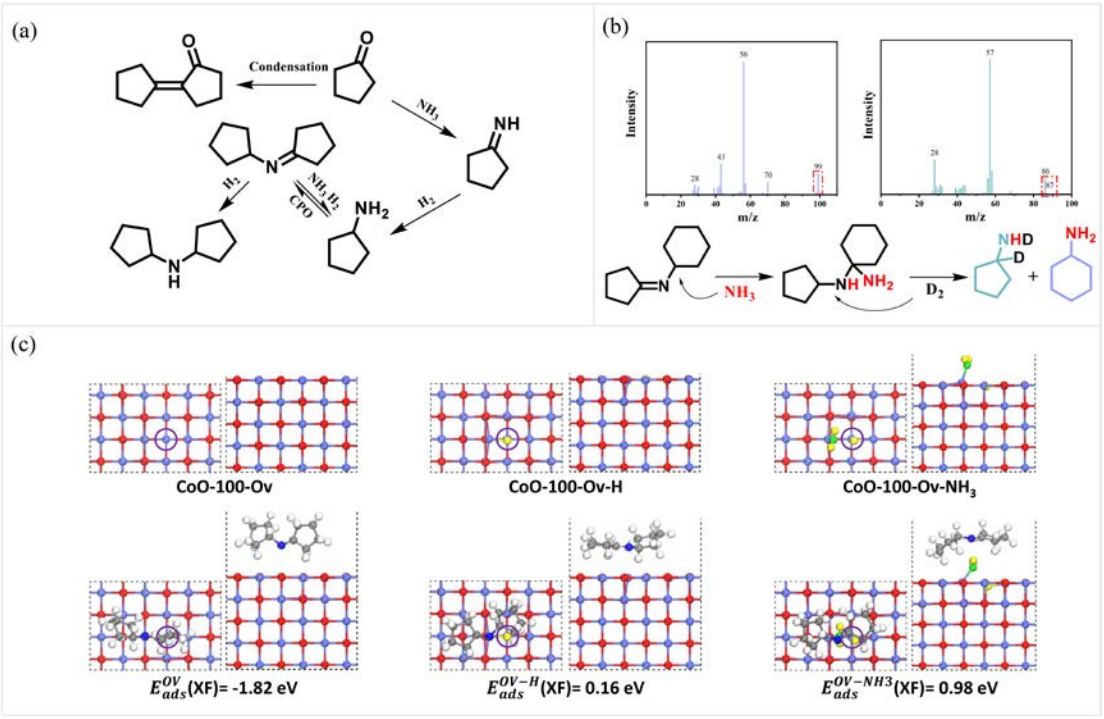

Fig. 4. (a) The possible reaction route for amination of cyclopentanone (CPO). (b) Schiff bases ammonolysis under D_2. (c) Calculated adsorption structures of Schiff baseon reduced CoO (100) surfaces. (Schiff base, H^-+Schiff base and $NH_2^{\delta-}{}_{ads}$ + Schiff base).

The following emphasis was placed on the exploration of the unique role of the hydride-like $NH_2^{\delta-}$ species. The time course (Figure S1) shows that the yield of Schiff base tends to increase at the first 4h, then gradually converts into target product, cyclopentylamine with the prolonging of reaction time. It indicates that the Schiff base is indeed the key intermediate and its further conversion is able to determine the whole rate of the reductive amination. Previous reports revealed that the conversion of Schiff base into primary amine includes two steps, namely the addition of Schiff bases with NH_3 to geminal diamine and subsequent

hydrogenolysis to produce primary amine (Figure 4a).[15] Hydrogen-deuterium exchange experiments were conducted to understand the reaction mechanism (Figure 4b). Under D_2 and NH_3, the Schiff bases were converted into cyclohexylamine and two deuteriums-isotopic cyclopentylamine. The molecular ion peak of cyclopentylamine (CPA) has increased from 85 to 87, suggesting that D_2 was added into the C=N group of Schiff base. We speculate that the H of -NHD is not stable, so the fragment peak at 87 was extremely weak and the fragment peak at 86 was stronger (Figure 4b). Clearly, no D_2 attacked the cyclohexane part, indicating that the $NH_2^{\delta-}$ species attacked the C^+ position of C-N, instead of C=N of Schiff base. This result confirmed that the $NH_2^{\delta-}$ species as an active hydride-like species indeed participated in the ammonolysis of Schiff base. To our knowledge, no evidence to prove the $H^{\delta-}$ species directly take part in the hydrogen/hydrogenolysis reaction was reported until now, although $H^{\delta-}$ species was believed to be highly active. Obviously, we provide convincing evidence that the hydride-like $NH_2^{\delta-}$species is directly involved in the reaction, which could indirectly indicate the $H^{\delta-}$ species involving the hydrogen/hydrogenolysis reaction and boost the research of H_2 heterolysis.

We are now in a position to elucidate the key role of the hydride-like $NH_2^{\delta-}$ species through DFT calculations (Figure 4c and Figure S2). With the introduction of H_2 and NH_3, three possible species including the clean CoO surface with oxygen vacancies (species **1**), the one formed via the adsorption of $H^{\delta-}$ species on the reduced CoO surface (species **2**) and the species from the co-adsorption of $H^{\delta-}$ and $NH_2^{\delta-}$ species on the reduced CoO surface (species **3**) exist in reaction system (Figure 4c). Comparison of adsorption energy of three species demonstrates that species **3** is of distinctive advantage in thermodynamics, implying that the homolytic

cleavage of NH_3 to $NH_2^{\delta-}$ and H^- occurs easily to generate the most stable intermediate to drive the following catalytic cycle. Furthermore, we quantitatively calculated the adsorption energies of Schiff base on the three intermediates. The results show that the adsorption on species **3** is strongly endothermic by 0.98 eV, larger than that on species **2** (0.16 eV). By marked contrast, 1.82 eV is released when the adsorption sites resided on species **1**. These calculations disclose that species **3** afford the weakest adsorption to Schiff base. It is therefore reasonable to believe that the extremely weak adsorption allows the Schiff base to move freely on the surface of the stable species **3**, providing an in-depth explanation of why hydride-like $NH_2^{\delta-}$ species can facilitate the reductive amination such uniquely from molecule collision theory.

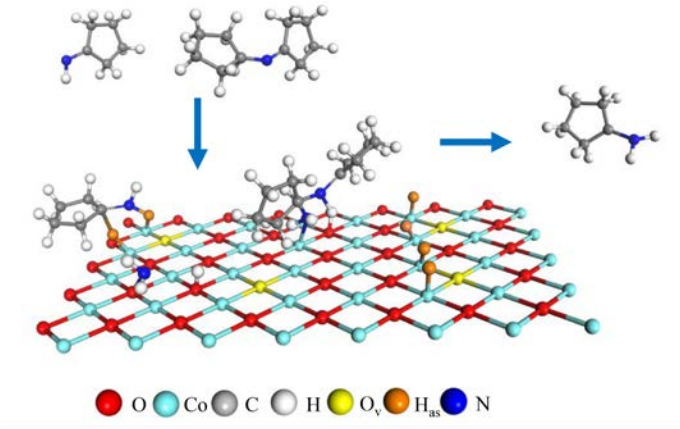

Fig. 5. The possible reaction mechanism of imine hydrogenation and aminolysis of Schiff base.

Based on the above results, we proposed the mechanism of the ammonolysis of Schiff base (Figure 5). Firstly, the dissociated the hydride-like $NH_2^{\delta-}$ species and H^- over Co@CoO attacked the C and N atoms on C−N groups of Schiff base, respectively, thus forming the corresponding geminal diamine. Then the H^- species from H_2 attacked the C atom of C=N groups to produce primary amines, respectively. The CoO shell not only drives the dissociation of H_2 to active $H^{\delta-}$ species but also enables the homolytic cleavage of NH_3.

Conclusion

In summary, a hydride-like $NH_2^{\delta-}$ species-driven reductive amination was reported and this unique $NH_2^{\delta-}$ species was generated from the dissociation of NH_3 over the CoO shell of core-shell structured Co@CoO catalyst. This unique $NH_2^{\delta-}$ species gives Co@CoO enormous power to convert various substrates to produce corresponding primary amines. This catalyst exhibits considerable performance and excellent stability compared to other emerging metal catalysts during the reductive amination. We revealed that the stable intermediate formed through the co-adsorption of $H^{\delta-}$ and $NH_2^{\delta-}$ species affords the extremely weak adsorption to Schiff base, accordingly allowing the Schiff base highly active in the molecular collision to present the desired reactivity. This work offers a new insight into the role of hydride-like $NH_2^{\delta-}$ species and deepens the understanding of the dissociation of these hydride-like species involved in many other important reactions.

Methods

Catalyst preparation

Co_3O_4 was synthesized with a precipitation method. Cobalt nitrate is used as the synthetic precursor. In the typical process, 60 mmol of cobalt nitrate and 69 mmol of $(NH_4)_2CO_3$ was dissolved in 200 ml distilled water, respectively. Then the solution of $(NH_4)_2CO_3$ was added dropwise into the aqueous solution of cobalt salt under vigorous stirring until the pH of the mother liquid reached approximately 8.5. Finally, the suspension was aged at 65 °C for 1 h with stirring and then left to stand at room temperature for 12h. After filtration and thoroughly washed with distilled water, the solid product was dried at 100 °C for 12 h and then calcined in air at 450 °C for 4h to obtain Co_3O_4.

The as-prepared Co_3O_4 was further reduced at desired temperature (250 °C) for 2 h under flowing H_2 (10% H_2-90% Ar mixed gas) in tube furnace with a ramp of 5 °C· min^{-1} before use. Thus-obtained reduced cobalt oxides were marked as Co@CoO.

Catalysts activity tests

The hydrogenation of propionamide was conducted in a Teflon-lined stainless-steel autoclave (50 mL). After sealing the desired dosage of propionamide, catalyst, and CH_3OH in the reactor, the autoclave was purged with NH_3 three times and pressurized to the desired pressure. After NH_3 purged, the H_2 was pressurized to the desired pressure. Then, the autoclave was heated to the predetermined temperature in a short time. After reaction, the reactor was quenched in an ice-water bath immediately.

The liquid phase was separated from the catalyst by centrifugation, and two individual GC/GC-MS systems were used for product analyses. The qualitative analysis of products was carried out on a GC-MS system (Agilent 7890A-5975C).

Catalyst characterization

Powder X-ray diffraction (XRD) patterns were recorded in the θ–2θ mode on a D8 Focus diffractometer (CuKα1 radiation, k=1.5406 Å), operated at 40 kV and 40 mA within scattering angels of 10–80°. Transmission electron microscopy (TEM) was obtained on a JEOL Model 2100 electron microscopy at 200 kV. The electron paramagnetic resonance (EPR) spectra were collected on a Bruker A300 spectrometer at 77 K.

Diffuse reflectance infrared Fourier transform spectra (DRIFTS) were recorded on a Nicolet Model iS-50 FT-IR spectrometer equipped with an MCT/A detector, and the sample cell was fitted with ZnSe windows. Diffuse reflectance infrared Fourier transform spectra (DRIFTS)

were recorded on a Nicolet Model iS-50 FT-IR spectrometer equipped with an MCT/A detector, and the sample cell was fitted with ZnSe windows. The DRIFT spectra were recorded with a resolution of 4 cm^{-1} and 32 scans. For the adsorption and activation of H_2/D_2 over Co@CoO catalyst, the as-prepared Co_3O_4 was loaded onto DRIFT IR cell, then reduce at 250 °C for 1 h under 10 % H_2−Ar mixed gas. After cooling down to 90 °C under Ar atmosphere, the spectrum was recorded as background. Then H_2 gas was imputed in the DRFIT cell at 90 °C for 40 min and the spectrum was recorded. Finally, D_2 gas was flushed into the cell at 90 °C for another 40 min to record the spectrum. The NH_3-DRIFT spectrum was also recorded in the similar procedure. Typically, after cooling down to 90°C, NH_3 gas was passed through the DRFIT cell for 5 min, then flushed with Ar at 90 °C for 20 min and recorded the spectrum.

Calculation Methods

In this work, all spin-polarized DFT calculations were carried out using the Vienna Ab–initio Simulation Package (VASP)[46]. The projector augmented wave (PAW) method[47] and the Perdew−Burke−Ernzerhof (PBE)[48] functional under the generalized gradient approximation (GGA)[49] were applied throughout the calculations. The kinetic energy cut-off was set to 400 eV, and the force threshold in structure optimization was 0.05 eV/Å. We used a large vacuum gap of 15 Å to eliminate the interactions between neighboring slabs. By adopting these calculation settings, the optimized lattice constant of CoO is 4.248 Å, which is in good agreement with the experimental value of 4.267 Å[50].

The adsorption energy of species X on the surface ($E_{ads}(X)$) was calculated with

$$E_{ads}(X) = E_{X/slab} - E_{slab} - E_X \qquad (1)$$

where $E_{X/slab}$ is the calculated total energy of the adsorption system, while E_{slab} and E_X are calculated energies of the clean surface and the gas phase molecule X, respectively. Obviously, a negative value of $E_{ads}(X)$ indicates an exothermic adsorption process, and the more negative the $E_{ads}(X)$ is, the more strongly the adsorbate X binds to the surface.

The oxygen vacancy formation energy (E_{OV}) was calculated according to

$$E_{OV} = E_{slab\text{-}OV} + 1/2E_{O2} - E_{slab} \quad (2)$$

where $E_{slab\text{-}OV}$ is the total energy of the surface with one oxygen vacancy, and E_{O2} is the energy of a gas phase O_2 molecule.

For the model construction, we built a *p*(2×3) surface slab containing five atomic layers for the CoO(100) surface, and the top four CoO layers of the CoO(100) were allowed to fully relax, while the bottom atomic layers were kept fixed to mimic the bulk region. A $2 \times 2 \times 1$ *k*-point mesh was used in calculations of all these models. Note that the on-site Coulomb interaction correction is necessary for the appropriate description of the Co 3*d* electrons, and all calculations are performed with U = 5.1 eV and J = 1.0 eV, which are consistent with the values determined by previous studies[51,52].

In addition, we tested the effect of the spin state of 3*d* electrons in Co^{2+} in the optimization of CoO, and found that the high-spin antiferromagnetic arrangement was the most stable state, and the calculated magnetic moment of 2.74 μB obtained from the difference in spin-up and spin-down densities is consistent with literature reports[53-55].

Date availability. The data supporting the findings of this study are available within the article, or available from the authors upon reasonable request.

References

1. Murugesan, K. *et al.* Catalytic reductive aminations using molecular hydrogen for synthesis of different kinds of amines. *Chem. Soc. Rev.* **49**, 6273-6328 (2020).
2. Froidevaux, V., Negrell, C., Caillol, S., Pascault, J.-P. & Boutevin, B. Biobased Amines: From Synthesis to Polymers; Present and Future. *Chem. Rev.* **116**, 14181-14224 (2016).
3. Afanasyev, O. I., Kuchuk, E., Usanov, D. L. & Chusov, D. Reductive Amination in the Synthesis of Pharmaceuticals. *Chem. Rev.* **119**, 11857-11911 (2019).
4. Senthamarai, T. et al. Simple ruthenium-catalyzed reductive amination enables the

synthesis of a broad range of primary amines. *Nat. Commun.* **9**, 4123 (2018).

5. Pelckmans, M., Renders, T., Van de Vyver, S. & Sels, B. F. Bio-based amines through sustainable heterogeneous catalysis. *Green Chem.* **19**, 5303-5331 (2017).
6. Niu, F. et al. A multifaceted role of a mobile bismuth promoter in alcohol amination over cobalt catalysts. *Green Chem.* **22**, 4270-4278 (2020).
7. Irrgang, T. & Kempe, R. Transition-Metal-Catalyzed Reductive Amination Employing Hydrogen. *Chem. Rev.* **120**, 9583-9674 (2020).
8. Gomez, S., Peters, J. A. & Maschmeyer, T. The Reductive Amination of Aldehydes and Ketones and the Hydrogenation of Nitriles: Mechanistic Aspects and Selectivity Control. *Adv. Synth. Catal.* **344**, 1037-1057 (2002).
9. Liang, G. *et al.* Production of Primary Amines by Reductive Amination of Biomass-Derived Aldehydes/Ketones. *Angew. Chem., Int. Ed.* **56**, 3050-3054 (2017).
10. Deng, D., Kita, Y., Kamata, K. & Hara, M. Low-Temperature Reductive Amination of Carbonyl Compounds over Ru Deposited on Nb2O5·nH2O. *ACS Sustain. Chem. Eng.* **7**, 4692-4698 (2019).
11. Qi, H. F. *et al*. Highly selective and robust single-atom catalyst Ru-1/NC for reductive amination of aldehydes/ketones. *Nat. Commun.* **12**, 3295 (2021).
12. Wang, T. *et al*. Rational design of selective metal catalysts for alcohol amination with ammonia. *Nat. Catal.* **2**, 773-779 (2019).
13. Pera-Titus, M. & Shi, F. Catalytic Amination of Biomass-Based Alcohols. *ChemSusChem* **7**, 720-722 (2014).
14. Guo, W., Tong, T., Liu, X., Guo, Y. & Wang, Y. Morphology-Tuned Activity of Ru/Nb2O5

Catalysts for Ketone Reductive Amination. *ChemCatChem* **11**, 4130-4138 (2019).

15. Dong, B. *et al.* Heterogeneous Ru-Based Catalysts for One-Pot Synthesis of Primary Amines from Aldehydes and Ammonia. *Catalysts* **5**, 2258-2270 (2015).
16. Nishimura, S., Mizuhori, K. & Ebitani, K. Reductive amination of furfural toward furfurylamine with aqueous ammonia under hydrogen over Ru-supported catalyst. *Res. Chem. Intermed.* **42**, 19-30 (2016).
17. Komanoya, T., Kinemura, T., Kita, Y., Kamata, K. & Hara, M. Electronic Effect of Ruthenium Nanoparticles on Efficient Reductive Amination of Carbonyl Compounds. *J. Am. Chem. Soc.* **139**, 11493-11499 (2017).
18. Nakamura, Y., Kon, K., Touchy, A. S., Shimizu, K.-I. & Ueda, W. Selective Synthesis of Primary Amines by Reductive Amination of Ketones with Ammonia over Supported Pt catalysts. *ChemCatChem* **7**, 921-924 (2015).
19. Liang, G. *et al*. Production of Primary Amines by Reductive Amination of Biomass-Derived Aldehydes/Ketones. *Angew. Chem., Int. Ed.* **129**, 3096-3100 (2017).
20. Chatterjee, M., Ishizaka, T. & Kawanami, H. Reductive amination of furfural to furfurylamine using aqueous ammonia solution and molecular hydrogen: an environmentally friendly approach. *Green Chem.* **18**, 487-496 (2016).
21. Haskelberg, L. Aminative Reduction of Ketones. *J. Am. Chem. Soc*. **70**, 2811-2812 (1948).
22. Murugesan, K., Beller, M. & Jagadeesh, R. V. Reusable Nickel Nanoparticles-Catalyzed Reductive Amination for Selective Synthesis of Primary Amines. *Angew. Chem., Int. Ed.* **58**, 5064-5068 (2019).
23. Hahn, G., Kunnas, P., De Jonge, N. & Kempe, R. General synthesis of primary amines via

reductive amination employing a reusable nickel catalyst. *Nat. Catal.* **2**, 71-77 (2019).

24. Yuan, H. et al. Reductive Amination of Furanic Aldehydes in Aqueous Solution over Versatile NiyAlOx Catalysts. *ACS Omega.* **4**, 2510-2516 (2019).
25. Chen, W. *et al*. Preparation of 5-(Aminomethyl)-2-furanmethanol by direct reductive amination of 5-Hydroxymethylfurfural with aqueous ammonia over the Ni/SBA-15 catalyst. *J. Chem. Technol. Biotechnol.* **93**, 3028-3034 (2018).
26. Jagadeesh, R. V. *et al*. MOF-derived cobalt nanoparticles catalyze a general synthesis of amines. *Science* **358**, 326-332 (2017).
27. Senthamarai, T. *et al*. Ultra-small cobalt nanoparticles from molecularly-defined Co–salen complexes for catalytic synthesis of amines. *Chem. Sci.* **11**, 2973-2981 (2020).
28. Zhuang, X., Liu, J., Zhong, S. & Ma, L. Selective catalysis for the reductive amination of furfural toward furfurylamine by graphene-co-shelled cobalt nanoparticles. *Green Chem.* **24.** 271-284 (2022).
29. Jagadeesh, R. V. et al. MOF-derived cobalt nanoparticles catalyze a general synthesis of amines. *Science* **358**, 326 (2017).
30. Lent, R. v. *et al.* Site-specific reactivity of molecules with surface defects—the case of H2 dissociation on Pt. *Science* **363**, 155-157 (2019).
31. Liu, P. *et al*. Photochemical route for synthesizing atomically dispersed palladium catalysts. *Science* **352**, 797-800 (2016).
32. Ye, T.-N. *et al*. Stable single platinum atoms trapped in sub-nanometer cavities in 12CaO·7Al2O3 for chemoselective hydrogenation of nitroarenes. *Nat. Commun.***11**, 1020 (2020).

33. Li, S. *et al*. Selective hydrogenation of 5-(hydroxymethyl)furfural to 5-methylfurfural over single atomic metals anchored on Nb2O5. *Nat. Commun.***12**, 584 (2021).

34. Zhang, S. *et al*. Solid frustrated-Lewis-pair catalysts constructed by regulations on surface defects of porous nanorods of CeO2. *Nat. Commun.* **8**, 15266 (2017).

35. 35 Zhang, Z. *et al*. Metal-Free Ceria Catalysis for Selective Hydrogenation of Crotonaldehyde. *ACS Catal.* **10**, 14560-14566 (2020).

36. Xiang, S. *et al.* Co@CoO: a Unique Catalyst for Hydrogenolysis of Biomass-derived 5-Hydroxymethylfurfural to 2,5-Dimethylfuran. DOI:10.26434/chemrxiv-2021-tjsr8.

37. Ramis, G. *et al.* Adsorption, Activation, and Oxidation of Ammonia over SCR Catalysts. *J. Catal.* **157**, 523-535 (1995).

38. Tamm, S., Vallim, N., Skoglundh, M. & Olsson, L. The influence of hydrogen on the stability of nitrates during H-2-assisted SCR over Ag/Al2O3 catalysts - A DRIFT study. *J. Catal.* **307**, 153-161 (2013).

39. Sun, D., Liu, Q., Liu, Z., Gui, G. & Huang, Z. Adsorption and oxidation of NH3 over V2O5/AC surface. *Appl. Catal., B* **92**, 462-467 (2009).

40. Tsyganenko, A. A., Pozdnyakov, D. V. & Filimonov, V. N. Infrared study of surface species arising from ammonia adsorption on oxide surfaces. *J. Mol. Struct.* **29**, 299-318 (1975).

41. Zhu, Y., Zhang, Y., Xiao, R., Huang, T. & Shen, K. Novel holmium-modified Fe-Mn/TiO2 catalysts with a broad temperature window and high sulfur dioxide tolerance for low-temperature SCR. *Catal. Commun.* **88**, 64-67 (2017).

42. Klukowski, D. *et al.* On the mechanism of the SCR reaction on Fe/HBEA zeolite. *Appl. Catal., B* **93**, 185-193 (2009).

43. Elfinger, M. *et al*. Co-Catalyzed Synthesis of Primary Amines via Reductive Amination employing Hydrogen under very mild Conditions. *ChemSusChem* **14**, 2360-2366 (2021).

44. Bäumler, C., Bauer, C. & Kempe, R. The Synthesis of Primary Amines through Reductive Amination Employing an Iron Catalyst. *ChemSusChem* **13**, 3110-3114 (2020).

45. Zhou, K. *et al.* Selective Synthesis of Furfurylamine by Reductive Amination of Furfural over Raney Cobalt. *ChemCatChem* **11**, 5562-5569 (2019).

46. Kresse, G. *et al*. Efficient iterative schemes for ab initio total-energy calculations using a plane-wave basis set. *Phys. Rev. B* **54**, 11169-11186 (1996).

47. Blöchl, P. E. Projector augmented-wave method. *Phys. Rev. B* **50**, 17953-17979 (1994).

48. Perdew, J. P. *et al*. Generalized gradient approximation made simple. *Phys. Rev. Lett*. **77**, 3865-3868 (1996).

49. Teter, M. P. *et al*. Solution of schrodinger's equation for large systems. *Phys. Rev. B* **40**, 12255-12263 (1989).

50. Redman, M. J. *et al*. Cobaltous oxide with the zinc blende/wurtzite-type crystal structure. *Nature* **193**, 867-867 (1962).

51. Archer, T. *et al*. Magnetism of CoO polymorphs: density functional theory and monte carlo simulations. *Phys. Rev. B* **78**, 014431(2008).

52. Pickett, W. E. *et al*. Reformulation of the LDA+U method for a local-orbital basis. *Phys. Rev. B* **58**, 1201-1209 (1998).

53. Solovyev, I. V. *et al*. Is hund's second rule responsible for the orbital magnetism in solids? *Phys. Rev. Lett*. **80**, 5758-5761 (1998).

54. Rödl, C. *et al*. Quasiparticle band structures of the antiferromagnetic transition-metal

oxides MnO, FeO, CoO, and NiO. *Phys. Rev. B* **79**, 235114 (2009).

55. Wdowik, U. D. *et al*. Lattice dynamics of CoO from first principles. *Phys. Rev. B* **75**, 104306 (2007).

Acknowledgments

The authors thank the financially supports by the NSFC of China (21832002, 21825301, 22072042, 22172048 and 22102056) and the China Postdoctoral Science Foundation (2021M691011 and 2021TQ0106).

Author Contributions

Y.Q.W. and Y.X.J. conceived and supervised the project. W.J.G. and Y.Q.W. designed experiments. W.J.G., X.S. and Y.X.J. performed the synthesis, characterisation, catalytic testing and process analysis. Z.Q.W. X.Q.G and Y.X.J. conducted DFT simulation of Schiff base, H_2 and NH_3 over CoO (1 0 0). Y.G. and X.H.L. participated in analysis of DRIFT of H/D and NH_3. W.J.G., Y.X.J. and Y.Q.W. wrote the manuscript. All authors participated in discussions and paper preparation.

Competing interests

The authors declare no competing financial interest.